Journal of Photochemistry and Photobiology A: Chemistry 216 (2010) 94–103

Contents lists available at ScienceDirect

Journal of Photochemistry and Photobiology A: Chemistry

journal homepage: www.elsevier.com/locate/jphotochem

Photoinduced electron transfer from Ru am(m)ine compounds with low-lying ligand field excited states to nanocrystalline TiO_2

Hai-Long Xia[a], Feng Liu[a], Shane Ardo[a], Amy A. Narducci Sarjeant[a], Gerald J. Meyer[a,b,*]

[a] Department of Chemistry, Johns Hopkins University, Baltimore, MD 21218, United States
[b] Department of Materials Science and Engineering, Johns Hopkins University, Baltimore, MD 21218, United States

ARTICLE INFO

Article history:
Available online 6 July 2010

Keywords:
Photochemistry
Excited states
Interfacial
Electron transfer

ABSTRACT

The coordination compounds $[Ru(NH_3)_5(eina)](PF_6)_2$, $[Ru(NH_3)_4(deeb)](PF_6)_2$ and $[Ru(en)_2(deeb)](PF_6)_2$, where eina is ethyl isonicotinate, deeb is 4,4′-$(CO_2CH_2CH_3)_2$-2,2′-bipyridine and en is ethylenediamine, were synthesized and characterized. $[Ru(NH_3)_4(deeb)](PF_6)_2{\cdot}2CH_3COCH_3$ and $[Ru(en)_2(deeb)](PF_6)_2{\cdot}CH_3COCH_3$ single crystals were characterized by X-ray crystallography. Near-infrared photoluminescence was observed after photoexcitation of $[Ru(en)_2(deeb)](PF_6)_2$ in butyronitrile at 77 K. The excited states of these compounds were found to be short-lived in fluid solution and when anchored to mesoporous nanocrystalline (anatase) TiO_2 thin films immersed in CH_3CN at room temperature, consistent with excited-state lifetimes <10 ns. Prolonged steady-state visible light excitation of the compounds in fluid solution and when anchored to ZrO_2 films immersed in CH_3CN resulted in a loss of the metal-to-ligand charge transfer (MLCT) absorption that was attributed to ligand-field photochemistry. Pulsed 532 nm light excitation of the compounds anchored to TiO_2 thin films yielded an interfacial charge-separated state, *i.e.* $Ru^{III}/TiO_2(e^-)$, that formed within 10 ns and returned cleanly to the initial Ru^{II}/TiO_2 state on a micro- to milli-second time scale. Quantum yields for formation of this state determined by comparative actinometry were excitation wavelength dependent suggesting the involvement of "hot" MLCT excited states. The quantum yields were also dependent on acid/base pre-treatments of the TiO_2 surface. Photoelectrochemical performances of $[Ru(NH_3)_4(deeb)](PF_6)_2$ and $[Ru(en)_2(deeb)](PF_6)_2$ on TiO_2 in regenerative solar cells were consistent with excitation-wavelength-dependent electron injection.

1. Introduction

Interfacial excited-state electron injection at dye-sensitized anatase TiO_2 nanoparticles has been shown to take place on femto- to pico-second time scales under a variety of experimental conditions [1]. The femtosecond component suggests that interfacial electron injection occurs from the initially populated Franck–Condon state and/or vibrationally "hot" excited states that compete kinetically with vibrational cooling, intersystem crossing, or radiative and non-radiative decay [2]. Therefore, sensitizers with short-lived, non-emissive excited states can be envisioned for energy-conversion applications at these interfaces. Indeed, several groups including our own have sensitized TiO_2 to visible light with transition-metal coordination compounds that have short-lived excited states [3]. A common motivation for this research is to replace the standard Ru(II) polypyridyl sensitizers with less expensive coordination compounds based on iron. The rapid deactivation of metal-to-ligand charge transfer (MLCT) excited states by low-lying ligand field (LF) excited states in iron polypyridyl compounds has historically limited their application in solar energy conversion. Indeed LF excited states typically yield unwanted and irreversible photochemistry.

In many respects, the excited states of Ru(II) compounds with weak-field ligands resemble those of Fe(II). A case in point are Ru(II) pyridyl ammine compounds that display MLCT-like emission at low temperatures but are highly quenched and susceptible to photo-induced ligand loss under ambient conditions [4,5]. For example, Ford and co-workers have reported systematic photo-aquation investigations of compounds of the general type $Ru(NH_3)_4(py')^{2+}$, where py′ is pyridine or a substituted pyridine. The observation of excitation wavelength dependent quantum yields for this photochemistry indicated less than unity intersystem crossing. Competitive surface crossing from the ^{1}MLCT to a LF excited state was proposed [4]. The lowest lying excited states of these compounds were LF in nature when the absorption maximum was roughly >460 nm and was MLCT when the maximum was <460 nm.

* Corresponding author at: Department of Chemistry, Johns Hopkins University, Baltimore, MD 21218, United States. Tel.: +1 1 410 516 7319; fax: +1 1 410 516 8420.
E-mail address: meyer@jhu.edu (G.J. Meyer).

1010-6030/$ – see front matter © 2010 Elsevier B.V. All rights reserved.
doi:10.1016/j.jphotochem.2010.06.035

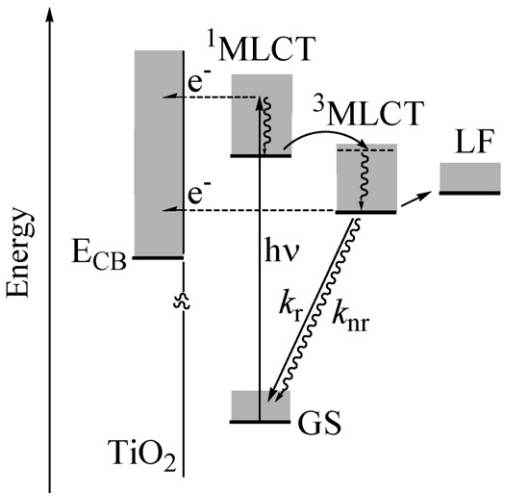

Fig. 1. A simplified representation of possible relaxation pathways from the metal-to-ligand charge-transfer (MLCT) excited states of Ru(II) ammine compounds anchored to anatase TiO_2. Both the ^{1}MLCT and thermally equilibrated triplet excited (thexi) state, ^{3}MLCT, may inject electrons into TiO_2 in competition with radiative and non-radiative decay and population of low-lying ligand field (LF) excited states.

When ruthenium ammine compounds are anchored to TiO_2 films, these intramolecular relaxation processes, *i.e.* vibrational cooling, internal conversion, intersystem crossing and/or thermally activated LF state population, may be expected to compete kinetically with excited-state electron injection, Fig. 1 [1,6]. Since electron injection has been shown to occur from vibrationally "hot" MLCT excited state but remains unprecedented for LF excited states, variation of the excitation wavelength may change the branching ratios between interfacial electron injection and intramolecular relaxation processes. Thus the efficiency of excited-state electron injection was expected and found to be wavelength dependent. For example, the excited-state electron injection quantum yield from $[Ru(NH_3)_5(eina)](PF_6)_2$, where eina is ethyl isonicotinate, was found to be ~30% with 416 nm light excitation and about half that with 532 nm light excitation. However, the energetics of the $Ru^{III/II}$ reduction potential resulted in sluggish iodide oxidation and poor solar cell efficiency [6].

In this manuscript, two new ruthenium am(m)ine compounds, $[Ru(NH_3)_4(deeb)](PF_6)_2$ and $[Ru(en)_2(deeb)](PF_6)_2$, where deeb is 4,4′-$(CO_2CH_2CH_3)_2$-2,2′-bipyridine and en is ethylenediamine, were prepared, characterized and anchored to mesoporous nanocrystalline TiO_2 thin films. X-ray crystal structures, solvatochromism, low temperature photoluminescence, and interfacial electron transfer behaviors are described. The aim of this work was to study the excitation wavelength dependence of the processes shown schematically in Fig. 1. The photocurrent responses of sensitized TiO_2 thin films in regenerative solar cells were quantified and found to be consistent with excitation-wavelength-dependent electron injection.

2. Materials and methods

2.1. Materials

[$Ru(NH_3)_6]Cl_3$ and $RuCl_3{\cdot}xH_2O$ were used as received from Alfa Aesar. Tetrabutylammonium perchlorate ($TBAClO_4$) (≥98%) was from Fluka and recrystallized from ethanol before use. Ligand deeb was prepared as previously described [7]. $[Ru(NH_3)_5Cl]Cl_2$ was prepared according to literature methods [8]. All other chemicals were used as received without purification. All solvents for synthesis and purification were of reagent grade or better.

Mesoporous nanocrystalline (anatase) TiO_2 thin (8–10 μm) films were prepared by a sol–gel technique that has been previously described [9]. For photoelectrochemical measurements the TiO_2 particles were coated on conductive fluorine-doped tin oxide (FTO) glass (Hartford Glass Co., Inc.; 15 Ω/square). For spectroscopic measurements, the anatase particles were coated on glass microscope slides (Fisher Scientific). In most experiments the thin films were pre-treated with aqueous solutions of known pH for 30 min, rinsed with neat acetonitrile, dried under vacuum and then exposed to mM concentrations of the Ru(II) compounds in acetonitrile in the dark [10]. The pH was adjusted with H_2SO_4 or NaOH aqueous solution.

2.2. Sensitizer synthesis

$[Ru(NH_3)_5(eina)](PF_6)_2$ was prepared by a method similar to that reported by Ford, et al. [11]. A 0.3 g of $[Ru(NH_3)_5Cl]Cl_2$ was digested at 50 °C with 4.2 mL of 0.5 M silver trifluoroacetate aqueous solution to give chloro penta-ammine-ruthenium(III) trifluoroacetate. After filtration, the filtrate was reduced by freshly prepared zinc amalgam under argon for 25 min. The resulting pale yellow $[Ru^{II}(NH_3)_5(OH_2)]^{2+}$ solution was transferred anaerobically to an argon-filled flask containing 20 mL of 1:1 H_2O/EtOH (v/v) with 1 mL of eina. A deep red color immediately formed. After 1 h in the dark at room temperature, solvent and unreacted eina were evaporated under vacuum. The solid was dissolved in 25 mL of deaerated H_2O and filtered on a fine frit. To the filtrate was added 2 mL of saturated NH_4PF_6 aqueous solution and the resulting red-orange precipitate was collected and subsequently washed twice with 5 mL of cold water. The product was stored under vacuum in the dark until use. ^{1}H NMR δ (ppm), CD_3CN: 8.63 (2H, d, J = 5.6 Hz), 7.71 (2H, d, J = 5.4 Hz), 4.41 (2H, q, J = 7.1 Hz), 2.63 (~5H, s), 1.42 (3H, t, J = 7.0 Hz).

2.2.1. $[Ru(NH_3)_4(deeb)](PF_6)_2$

$[Ru(NH_3)_4(deeb)](PF_6)_2$ was synthesized via a slightly modified literature method [12]. Several milliliters of freshly prepared aqueous $[Ru^{II}(NH_3)_5(OH_2)]^{2+}$ solution was transferred anaerobically to an argon-filled flask containing 0.92 equivalent of deeb in 1:2 (v/v) H_2O/EtOH (v/v). After 4 h at 60 °C in the dark, the volume of solvents was reduced under an argon flow at room temperature. The solution was filtered on a fine frit and water was then added to the filtrate to reach a final volume of ~20 mL. A brown precipitate was obtained after 2 mL of saturated aqueous NH_4PF_6 solution was added. The precipitate was collected and washed with cold water and dried under vacuum. The compound was dissolved in a minimum amount of acetone and purified on a Sephadex LH-20 column with acetone as the eluent. Dark brown crystals suitable for X-ray diffraction were then recrystallized from acetone–ether mixtures. ^{1}H NMR δ (ppm), CD_3COCD_3: 9.57 (2H, d, J = 6.1 Hz), 8.94 (2H, d, J = 2.0 Hz), 7.94 (2H, dd, J = 2.0 Hz, J = 2.0 Hz), 4.48 (4H, q, J = 7.1 Hz), 3.74 (6H, s) 2.32 (6H, s), 1.42 (6H, t, J = 7.1 Hz).

2.2.2. $[Ru(en)_2(deeb)](PF_6)_2$

The double salt $[Ru(en)_2(ox)][Ru(en)(ox)_2]$ was prepared as previously described, where ox is oxalate [13]. Attempts to convert the double salt directly to $[Ru(en)_2Cl_2]Cl$ with concentrated HCl were unsuccessful. Instead, the double salt was reacted with sodium tetraphenylborate aqueous solution at room temperature for 30 min and filtered. The precipitate was collected and dissolved in 12 M HCl (1 g of complex in 10 mL of 12 M HCl) at 50 °C and stirred for 1 h. The mixture was then filtered and the filtrate was evaporated to dryness. The resulting product $[Ru(en)_2Cl_2]Cl$ was washed by cold ethanol and acetone. $[Ru(en)_2Cl_2]Cl$ was digested with silver trifluoroacetate aqueous solution and filtered. The filtrate was reduced with amalgamated mossy zinc for 15 min and

the resulting ruthenium(II) solution was transferred anaerobically to an argon-filled flask containing 0.92 equivalent of deeb in 25 mL of 1:2 H_2O/EtOH (v/v). The reaction was carried out at 60 °C in the dark for 5 h. Precipitation and recrystallization steps were the same as those for the preparation of $[Ru(NH_3)_4(deeb)](PF_6)_2$. Dark brown crystals suitable for X-ray diffraction were obtained. ^{1}H NMR δ (ppm), CD_3CN: 9.20 (2 H, d, J = 6.1 Hz), 8.85 (2H, s), 7.95 (2H, d, J = 6.1 Hz), 4.49 (4H, q, J = 7.2 Hz), 4.26 (2H, m), 3.94 (2H, m), 3.28 (2H, m), 2.93 (2H, m), 1.46 (6H, t, J = 7.2 Hz).

2.3. Measurements

2.3.1. X-ray crystallography

Crystals of $[Ru(NH_3)_4(deeb)](PF_6)_2{\cdot}2CH_3COCH_3$ and $[Ru(en)_2(deeb)](PF_6)_2{\cdot}CH_3COCH_3$ were obtained by slow diffusion of diethyl ether into an acetone solution of the compounds. Intensity data were measured with Mo Kα radiation, λ = 0.71073 Å, at 110 K on an Oxford Diffraction Xcalibur3 system equipped with a graphite monochromator and a CCD detector. Data were collected via a series of 1.0° φ and ω scans. Face-indexed absorption and interframe scaling corrections were applied. The structures were solved by direct methods and were refined by full-matrix, least-squares methods, using the Bruker *SHELXTL* (version 6.1) software package, to yield final R and R_w values of 0.0750 and 0.2111 for $[Ru(NH_3)_4(deeb)](PF_6)_2{\cdot}2CH_3COCH_3$, and 0.0468 and 0.1078 for $[Ru(en)_2(deeb)](PF_6)_2{\cdot}CH_3COCH_3$. The PF_6^- anions appeared to be disordered and this lead to the high R value [14].

2.3.2. UV–vis (Vis) spectroscopy

All ground state absorption spectra were acquired at ambient temperature using a Hewlett–Packard 8453 diode array spectrophotometer. For sensitized films, the optical measurements were acquired by placing the TiO_2 slides diagonally in solvent-filled 10 mm × 10 mm quartz cuvette. An unsensitized TiO_2 film in a solvent-filled cuvette was used as the reference.

2.3.3. Adsorption isotherms

Surface binding was monitored spectroscopically by measuring the changes in film and solution absorbance after soaking the film for ∼16 h in acetonitrile solutions with known concentrations of the sensitizers. The equilibrium binding for all three compounds were well described by the Langmuir adsorption isotherm model from which surface binding constant (K_{ad}) was abstracted using Eq. (1):

$$\frac{[Ru^{II}]_{eq}}{\Gamma} = \frac{1}{K_{ad}\Gamma_0} + \frac{[Ru^{II}]_{eq}}{\Gamma_0} \quad (1)$$

where $[Ru^{II}]_{eq}$ is the equilibrium sensitizer concentration and Γ is the equilibrium surface coverage at a defined molar concentration. Plots of $[Ru^{II}]_{eq}/\Gamma$ vs. $[Ru^{II}]_{eq}$ were fitted linearly to obtain the adduct formation constant K_{ad} and saturation surface coverage Γ_0.

2.3.4. Photoluminescence

Low temperature emission spectra at 77 K in butyronitrile glasses were determined using a Princeton Instruments (Roper Scientific) OMAV/InGaAs array detector mounted on an Acton SP500 spectrometer as previously described [15]. The spectral response of the detection apparatus was calibrated with a NIST traceable Oriel Model 63358 Quartz Tungsten Halogen lamp.

2.3.5. Photoelectrochemistry

Photoelectrochemical and incident photon-to-current conversion efficiency (IPCE) measurements were performed in a two-electrode sandwich cell arrangement as previously described [6]. Briefly, ∼0.1 mL of electrolyte was sandwiched between a TiO_2 electrode and a Pt coated FTO electrode. For pH = 1 pre-treated TiO_2 slides, 0.5 M TBAI/0.05 M I_2 in CH_3CN was used as supporting electrolyte. The sensitized TiO_2 was illuminated with a 100 W Xe lamp coupled to an f/0.39 Oriel Cornerstone monochromator. Photocurrents were measured with a Keith Model 617 digital electrometer. Incident irradiances were measured with a calibrated silicon photodiode from UDT Technologies.

2.3.6. Electrochemistry

Cyclic voltammetry was performed in 0.1 M $TBAClO_4$ acetonitrile or dimethylformamide electrolyte. $TBAClO_4$ was recrystallized from ethanol and CH_3CN was distilled before use. A BAS Model CV27 potentiostat was used in a standard three-electrode arrangement consisting of a glassy carbon working electrode, a Pt gauge counter electrode and a Ag/AgCl reference electrode. The electrochemical measurements were performed in argon-saturated solutions. Cyclic voltammetry of the sensitizers bound to TiO_2 on an FTO conductive glass support was performed in a similar manner with the modified TiO_2 electrode as the working electrode.

2.3.7. Spectroelectrochemistry

Spectroelectrochemistry was performed for sensitizers in 0.1 M $TBAClO_4/CH_3CN$ solution. A local designed 1 mm path length quartz cuvette was used. A Pt mesh electrode was used as a working electrode while a $Ag/AgNO_3$ reference electrode and a Pt gauze auxiliary electrode were also employed. Potentials were applied with a PAR Model 173 potentiostat. The externally applied potential was usually about 200 mV positive of sensitizers' formal reduction potential. Argon was bubbled gently before and during the experiment. UV–vis spectra were obtained as needed. For sensitizers bound to TiO_2, spectroelectrochemistry was obtained using a sensitizer/TiO_2 film deposited on FTO glass as the working electrode.

2.3.8. Nanosecond transient absorption

Transient absorption data were acquired with a pulsed 150 W Xe lamp after pulsed-laser excitation from a Surelite II Nd:YAG (Q-switched ∼8 ns) laser frequency-doubled to 532 nm or -tripled to 355 nm followed by Stokes shifted to 416 nm with an H_2-filled Raman shifter, as has been previously described [6].

2.3.9. Interfacial electron injection quantum yield

The quantum yields for excited-state electron injection into TiO_2 were quantified by comparative actinometry as previously described [16]. A $[Ru(bpy)_3](PF_6)_2$ doped poly(methyl methacrylate) (PMMA) thin film, whose optical absorption and physical dimensions were very similar to the sensitized TiO_2 films, was used as the actinometer. The absorbance of the ground-state actinometer and the sensitized films were approximately matched at the excitation wavelength. A literature value of $(-1.00 \pm 0.09) \times 10^4\ M^{-1}cm^{-1}$ at 450 nm for the difference between the extinction coefficients of the excited-state and ground-state actinometer was used [16]. The extinction coefficients of the Ru(II) ground state and Ru(III) oxidation state were determined by Beer's law in solution and spectroelectrochemical measurements of the TiO_2-bound sensitizers, respectively.

2.3.10. Infrared

Fourier-transform infrared (FT-IR) spectra of the free and TiO_2-bound sensitizers were measured by attenuated total reflectance (ATR) with a Golden Gate Single Reflection Diamond ATR apparatus. KBr windows and unsensitized TiO_2 film were used as the backgrounds, respectively. The spectra were typically collected for 64 scans at 4 cm^{-1} resolution.

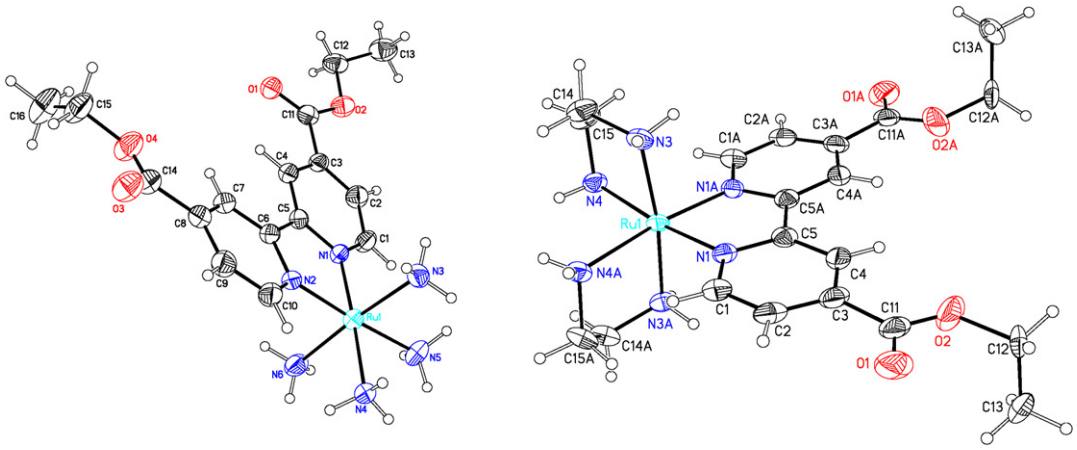

Fig. 2. ORTEP representations of $[Ru(NH_3)_4(deeb)]^{2+}$ (left) and $[Ru(en)_2(deeb)]^{2+}$ (right) with numbering scheme.

3. Results

The crystal structure of $[Ru(NH_3)_4(deeb)](PF_6)_2{\cdot}2CH_3COCH_3$ contains the cation, two disordered PF_6^- anions, and two acetone solvate molecules. Similarly, the solid-state structure of $[Ru(en)_2(deeb)](PF_6)_2{\cdot}CH_3COCH_3$ contains the cation, two PF_6^- anions, and one acetone solvate molecule. An ORTEP representation of the Ru(II) cations is shown in Fig. 2 and details of the crystal structure are given in Table 1. Selected bond distances and angles are listed in Table 2. The Ru centers are approximately octahedrally coordinated by nitrogen atoms from deeb and the am(m)ine ligands. The Ru–pyridyl nitrogen bond lengths, Ru–N_{pyr}, are considerably shorter than those to the am(m)ines, NH_3 or en. The Ru–N_{pyr} is even shorter than the corresponding value reported for $[Ru(NH_3)_4(bpy)](PF_6)_2{\cdot}0.5CH_3OH{\cdot}0.5H_2O$ [17]. Presumably, the Lewis basicity of the pyridyl nitrogens is decreased by the electron-withdrawing ethyl ester groups but this effect is offset by an increase in π acidity and hence a shorter and stronger Ru–N_{pyr} bond. The Ru–N_{am} bond distances are in fact longer for the am(m)ines that have trans pyridyl nitrogens. The two axial am(m)ine nitrogens are also slightly bent away from the deeb ligand with a N(3)–Ru(1)–N(6) bond angle 175.98(13)° in $[Ru(NH_3)_4(deeb)](PF_6)_2{\cdot}2CH_3COCH_3$, and a N(3)–Ru(1)–N(3A) angle of 172.58(19)° in $[Ru(en)_2(deeb)](PF_6)_2{\cdot}CH_3COCH_3$ (Table 2).

The visible absorption spectra of the three Ru(II) am(m)ine compounds were dominated by solvent-dependent MLCT absorption bands. Shown in Fig. 3 are the typical visible absorption spectra of $[Ru(en)_2(deeb)](PF_6)_2$ in acetonitrile and dimethylformamide. For $[Ru(NH_3)_5(eina)](PF_6)_2$, one absorption band was observed in the visible region assigned to Ru(II) → eina MLCT transitions. For $[Ru(NH_3)_4(deeb)](PF_6)_2$ and $[Ru(en)_2(deeb)](PF_6)_2$, two absorption bands were present, the lower and higher energy bands were assigned to the Ru(II) → deeb (LUMO) and Ru(II) → deeb (LUMO + 1), respectively, consistent with previous studies [18]. The optical and redox properties of the three ruthenium am(m)ine compounds in fluid solution are summarized in Table 3.

The molar extinction coefficients were approximately the same in acetonitrile and dimethylformamide, while the MLCT maxima significantly shifted to lower energies in dimethylformamide, Table 3 [3d,12b,19]. For example, the absorption maximum of $[Ru(NH_3)_5(eina)](PF_6)_2$ was 486 nm in acetonitrile and 530 nm in dimethylformamide (~1700 cm^{-1}). Similar spectral changes were observed with the tetra-am(m)ine compounds dissolved in these two solvents but the magnitude of the effect was smaller, typically ~25–30 nm (850–1350 cm^{-1}).

Room temperature equilibrium binding data of the ruthenium am(m)ine compounds to TiO_2 films in acetonitrile solution were fit to the Langmuir adsorption isotherm model from which surface adduct formation constants and limiting surface coverages were abstracted. The surface adduct formation constants were found to be dependent on the surface acidity. On base-treated TiO_2 samples the adduct formation constants were two to four times larger than those on acid-treated samples, Table 4. The adduct formation constant for $Ru(NH_3)_5(eina)^{2+}$ was larger than those measured

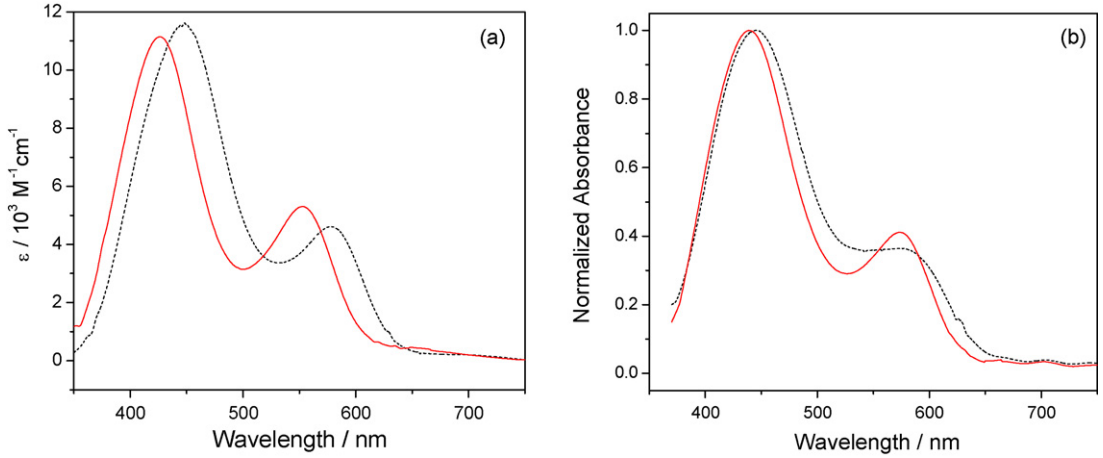

Fig. 3. Absorption spectra of $[Ru(en)_2(deeb)](PF_6)_2$ at room temperature: (a) in neat acetonitrile ( ) and dimethylformamide (—), and (b) anchored to TiO_2 thin films immersed in acetonitrile ( ) and dimethylformamide (—).

Table 1
Crystallographic data for $[Ru(NH_3)_4(deeb)](PF_6)_2{\cdot}2CH_3COCH_3$ and $[Ru(en)_2(deeb)](PF_6)_2{\cdot}CH_3COCH_3$.

	$[Ru(NH_3)_4(deeb)](PF_6)_2{\cdot}2CH_3COCH_3$	$[Ru(en)_2(deeb)](PF_6)_2{\cdot}CH_3COCH_3$
Formula	$C_{22}H_{40}F_{12}N_6O_6P_2Ru$	$C_{23}H_{38}F_{12}N_6O_5P_2Ru$
Crystal system	Triclinic	Monoclinic
Space group	*P*-1	*C*2/*c*
Temperature, K	110	110
a, Å	8.5533(8)	13.740(3)
b, Å	13.4392(13)	25.380(4)
c, Å	16.3339(14)	9.5661(13)
α,°	96.956(8)	90
β,°	94.438(7)	96.434(15)
γ,°	107.376(9)	90
Volume, Å^3	1765.9(3)	3314.9(10)
Z	2	4
d_{calc}, g/cm^3	1.647	1.742
Crystal size, mm	0.38512 × 0.16996 × 0.03328	0.2253 × 0.1013 × 0.0083
λ (Mo, Kα), Å	0.71073	0.71073
R ($I > 2\sigma(I)$)	0.0750	0.0468
R_w	0.2111	0.1078

Table 2
Selected bond distances (Å) and angles (°) for $[Ru(NH_3)_4(deeb)]^{2+}$ and $[Ru(en)_2(deeb)]^{2+}$.

$[Ru(NH_3)_4(deeb)]^{2+}$		$[Ru(en)_2(deeb)]^{2+}$	
Ru(1)–N(1)	2.024(3)	Ru(1)–N(1)	2.013(3)
Ru(1)–N(2)	2.022(3)	Ru(1)–N(1A)	2.013(3)
Ru(1)–N(3)	2.129(3)	Ru(1)–N(3)	2.108(3)
Ru(1)–N(4)	2.155(3)	Ru(1)–N(3A)	2.108(3)
Ru(1)–N(5)	2.131(3)	Ru(1)–N(4)	2.142(3)
Ru(1)–N(6)	2.130(4)	Ru(1)–N(4A)	2.142(4)
N(1)–Ru(1)–N(2)	79.92(12)	N(1)–Ru(1)–N(1A)	79.57(17)
N(1)–Ru(1)–N(3)	92.01(13)	N(1)–Ru(1)–N(3)	93.36(12)
N(1)–Ru(1)–N(4)	176.65(12)	N(1)–Ru(1)–N(3A)	92.34(12)
N(1)–Ru(1)–N(5)	96.58(13)	N(1)–Ru(1)–N(4)	173.36(12)
N(1)–Ru(1)–N(6)	90.92(14)	N(1)–Ru(1)–N(4A)	96.86(13)
N(2)–Ru(1)–N(3)	90.36(13)	N(1A)–Ru(1)–N(3)	92.34(12)
N(2)–Ru(1)–N(4)	96.78(13)	N(1A)–Ru(1)–N(3A)	93.36(13)
N(2)–Ru(1)–N(5)	175.98(13)	N(1A)–Ru(1)–N(4)	96.86(13)
N(2)–Ru(1)–N(6)	92.87(14)	N(1A)–Ru(1)–N(4A)	173.35(12)
N(3)–Ru(1)–N(4)	88.55(13)	N(3)–Ru(1)–N(3A)	172.58(19)
N(3)–Ru(1)–N(5)	87.79(14)	N(3)–Ru(1)–N(4)	81.13(13)
N(3)–Ru(1)–N(6)	175.98(13)	N(3)–Ru(1)–N(4A)	93.47(13)
N(4)–Ru(1)–N(5)	86.73(14)	N(3A)–Ru(1)–N(4)	93.47(13)
N(4)–Ru(1)–N(6)	88.69(14)	N(3A)–Ru(1)–N(4A)	81.13(13)
N(5)–Ru(1)–N(6)	89.13(15)	N(4)–Ru(1)–N(4A)	87.23(19)

for $Ru(NH_3)_4(deeb)^{2+}$ and $Ru(en)_2(deeb)^{2+}$. The visible absorption spectra for the compounds on TiO_2 were also found to be solvent dependent, though to a lesser extent than that observed in fluid solution. The visible spectrum of $[Ru(en)_2(deeb)](PF_6)_2$ on base pre-treated TiO_2 was typically red-shifted 5–10 nm relative to acid-treated TiO_2, Table 4. Absorption spectra observed on acid- or base-treated ZrO_2 films were qualitatively similar to those on TiO_2. The normalized absorption spectra of the three compounds in acetonitrile solutions used for surface binding did not change with time. No detectable room-temperature photoluminescence was measured from these compounds in solution or when anchored to TiO_2 or ZrO_2.

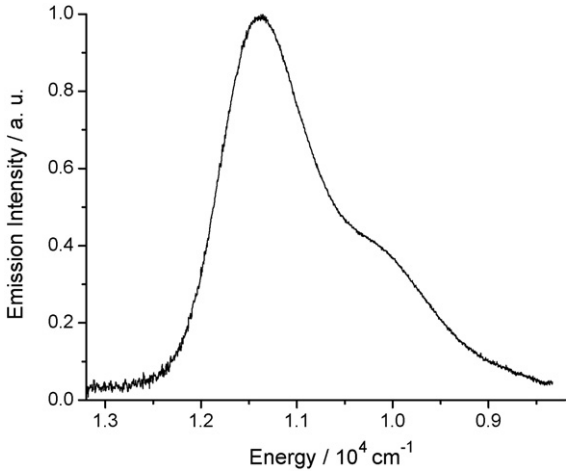

Fig. 4. Photoluminescence spectrum of $[Ru(en)_2(deeb)](PF_6)_2$ in a butyronitrile glass at 77 K.

Near-infrared photoluminescence measurements indicated that $[Ru(en)_2(deeb)](PF_6)_2$ was emissive at 77 K in butyronitrile glass with an MLCT emission maximum at ~11,400 cm^{-1}, Fig. 4. The spectrum showed evidence for a weak vibronic progression ($\nu \approx 1300\,cm^{-1}$) that is probably a convolution of many vibronic distortion modes. An approximately 6500 cm^{-1} pseudo-Stokes shift from the red MLCT absorption band in acetonitrile to the fundamental emission maximum was quantified that is similar to that reported for other tetra-am(m)ine ruthenium bipyridyl compounds [20]. No photoluminescence was observed for $[Ru(NH_3)_5(eina)](PF_6)_2$ under the same conditions, which was con-

Table 3
Photophysical and electrochemical properties of compounds.[a].

Compounds	λ_{abs}, nm ($\varepsilon \times 10^3$ M^{-1} cm^{-1})[b]		$h\nu_{em\ (max)}$ cm^{-1}[c]	$E_{1/2}(Ru^{III/II})$ mV[d]		$E_{1/2}$ ($L^{0/-}$) V[d]	
	ACN	DMF		ACN	DMF	ACN	DMF
$[Ru(NH_3)_5(eina)](PF_6)_2$	486 (14.7)	530 (13.7)	–	460	180	–	–
$[Ru(NH_3)_4(deeb)](PF_6)_2$	430 (10.4), 560	456 (10.8), 592	–	755	600	−1.28	−1.38
$[Ru(en)_2(deeb)](PF_6)_2$	424 (11.1), 552	448 (11.6), 580	11,400	830	650	−1.26	−1.35

[a] All measurements were made at 22 ± 2 °C, except emission measurements.
[b] ACN is acetonitrile and DMF is dimethylformamide. Absorption maxima are ±4 nm. Only absorption bands in the visible region are listed. The molar extinction coefficients are given in parentheses.
[c] In butyronitrile glass at 77 K.
[d] Potentials were reported vs. Ag/AgCl, ±20 mV, at a scan rate of 100 mV/s.

Table 4
Spectroscopic and redox properties, limiting surface coverages and equilibrium binding constants for Ru Am(m)ine compounds with acid- and base-pre-treated TiO_2 films at 22 ± 2 °C.

Compound	λ_{abs}, nm[a]				$E_{1/2}(Ru^{III/II})$, mV[b]				$\Gamma_0 \times 10^{-8}$ mol/cm^2		$K_{ad} \times 10^5$ M^{-1}	
	pH = 1 TiO_2		pH = 12 TiO_2		pH = 1 TiO_2		pH = 12 TiO_2		pH = 1 TiO_2	pH = 12 TiO_2	pH = 1 TiO_2	pH = 12 TiO_2
	ACN	DMF	ACN	DMF	ACN	DMF	ACN	DMF				
$Ru(NH_3)_5(eina)^{2+}$	505	555	528	558	172	−36	262	120	3 ± 2	10 ± 3	2.5	9.0
$Ru(NH_3)_4(deeb)^{2+}$	440	450	445	447	515	[c]	595	[d]	7 ± 2	9 ± 3	1.5	6.0
	580	595	595	600								
$Ru(en)_2(deeb)^{2+}$	440	445	440	443	730	[c]	800	[d]	8 ± 2	4 ± 1	1.2	3.0
	575	580	580	590								

[a] The acidity of the TiO_2 film refers to the acidity of the aqueous solution used to pre-treat the film. Measurements were made with an unsensitized TiO_2 film as reference. Absorption maxima are ±4 nm.
[b] Half-wave potentials were measured at an FTO/TiO_2/sensitizer working electrode in 0.1 M $TBAClO_4$ acetonitrile or dimethylformamide electrolyte for pH = 1 TiO_2 or in 0.1 M $LiClO_4$ acetonitrile or dimethylformamide electrolyte for pH = 12 TiO_2. Potentials were vs. Ag/AgCl.
[c] There was considerable desorption of the compounds from the surface.
[d] No clear cathodic peak currents were observed.

sistent with previous reports of ruthenium penta-ammine excited states measured at 4 K [21].

All compounds displayed quasi-reversible $Ru^{III/II}$ redox chemistry by cyclic voltammetry in fluid solution. The redox chemistry is termed quasi-reversible because the anodic and cathodic currents were approximately equal but the peak-to-peak separation was typically ~80–120 mV over scan rates of 20–100 mV/s [22]. For $Ru(NH_3)_4(deeb)^{2+}$ and $Ru(en)_2(deeb)^{2+}$, ligand-based half-wave reduction potentials, $E_{1/2}(L^{0/-})$, were also quantified, Table 3. Consistent with previous reports, the metal III/II half-wave reduction potentials, $E_{1/2}(Ru^{III/II})$, were highly solvent dependent while the ligand based reductions were only weakly solvent dependent [24]. In dimethylformamide, $E_{1/2}(Ru^{III/II})$ of $Ru(en)_2(deeb)^{2+}$ shifted 180 mV to 650 mV from 830 mV in acetonitrile. The first reduction potential of $Ru(en)_2(deeb)^{2+}$ shifted 90 mV from −1.26 V to −1.35 V when the solvent was changed from acetonitrile to dimethylformamide.

The sensitizers bound to acid- or base-treated TiO_2 electrodes displayed quasi-reversible $E_{1/2}(Ru^{III/II})$ in acetonitrile electrolyte. Positive shifts, ~70–90 mV, in the $Ru^{III/II}$ half-wave potentials between the pH = 1 and pH = 12 pre-treated surfaces in acetonitrile electrolyte were obtained for all the compounds. Considerable surface desorption and no clear cathodic peak currents were observed for $Ru(NH_3)_4(deeb)^{2+}$ and $Ru(en)_2(deeb)^{2+}$ on TiO_2 in the dimethylformamide electrolyte. For pH = 1 pre-treated samples with 0.1 M $TBAClO_4$ in either acetonitrile or dimethylformamide, the surface-bound sensitizers were stable in the formal oxidation states of II and III. Stepping the potential positive of $E_{1/2}(Ru^{III/II})$ resulted in oxidation of the surface-bound sensitizers that could be reversed by restoring the initial potential.

The 77 K photoluminescence spectrum from $Ru(en)_2(deeb)^{2+*}$ allows the free energy stored in the excited state to be estimated, ΔG_{es}, which can be used to calculate the excited-state reduction potential, $E_{1/2}(Ru^{III/II*})$, through the thermochemical cycle depicted with Eq. (2) [23]:

$$E_{1/2}(Ru^{III/II*}) = E_{1/2}(Ru^{III/II}) - \Delta G_{es} \quad (2)$$

Estimation of the excited-state reduction potential of $Ru(en)_2(deeb)^{2+*}$ anchored to acid pre-treated TiO_2 is thus −810 mV vs. Ag/AgCl, using the high-energy emission of the compound in solution at 77 K as an estimate of ΔG_{es}. We emphasize that it is an excited-state that injects the electron into TiO_2, and not the lowest unoccupied molecular orbital (LUMO) of the ground state.

FT-IR spectra of the solid compounds showed the presence of intense bands at ~1710–1725 cm^{-1} (ν_{COO}) for the carbonyl, ~1603 cm^{-1} (▬ ▬) for the aromatic ligand, and one band at ~1630 cm^{-1} for N–H scissoring. Upon surface binding to TiO_2 thin films, the asymmetric carboxylate stretch of $[Ru(NH_3)_4(deeb)](PF_6)_2$ shifted to higher energy, while there was no change for the same stretch of $[Ru(NH_3)_5(eina)](PF_6)_2$, within experimental error. Shown in Fig. 5a and b are the FT-IR spectra of $[Ru(NH_3)_5(eina)](PF_6)_2$ and $[Ru(NH_3)_4(deeb)](PF_6)_2$ bound to pH = 1 and pH = 12 pre-treated TiO_2, and the bands are summarized in Table 5. Interestingly, solid $[Ru(NH_3)_4(deeb)](PF_6)_2$ exhibited an intense band centered at 1710 cm^{-1}, while this bands

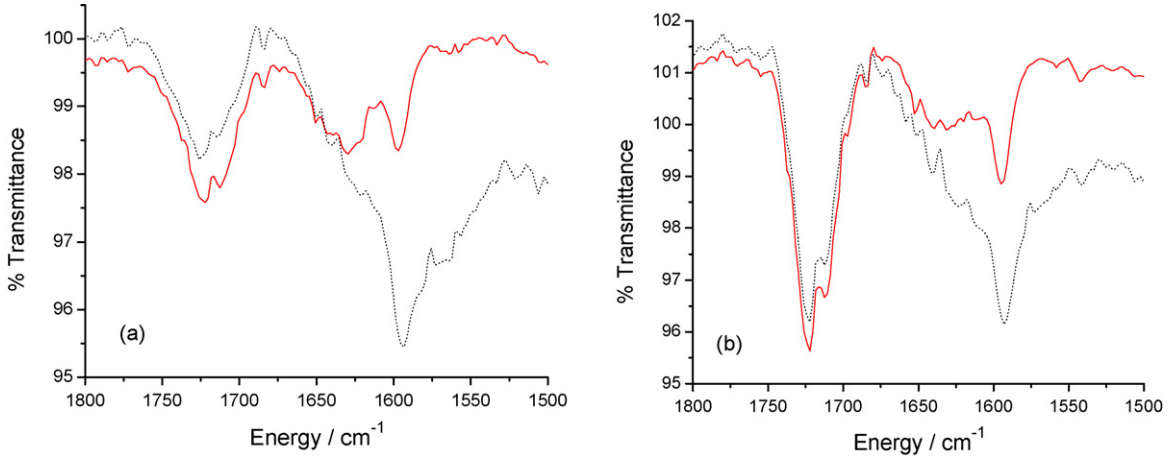

Fig. 5. Attenuated total reflectance spectra for (a) $Ru(NH_3)_5(eina)/TiO_2$, and (b) $Ru(NH_3)_4(deeb)/TiO_2$ with thin films that had been pre-treated with pH = 1 (▬) and pH = 12 (. . .) aqueous solutions.

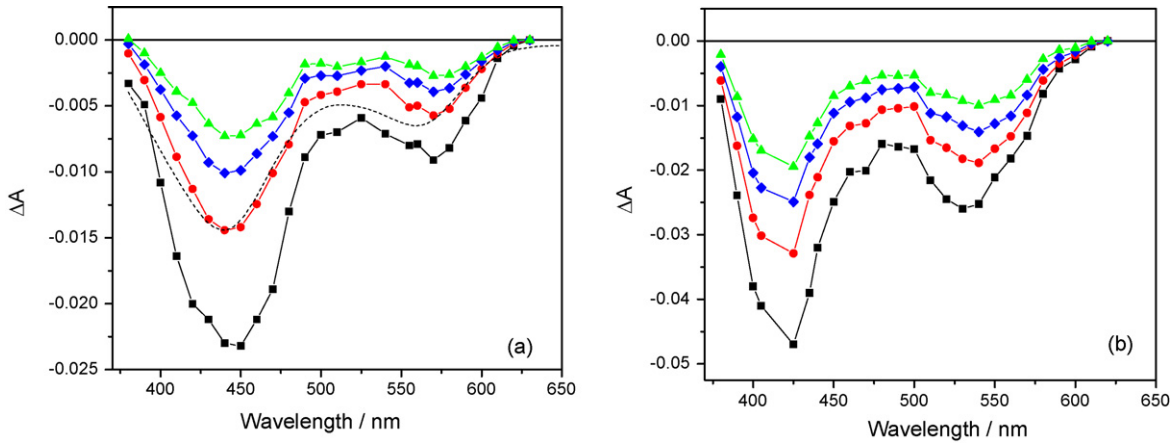

Fig. 6. Transient absorption difference spectra observed after 532 nm laser excitation (~10 mJ/pulse, 10 ns fwhm) of $Ru(en)_2(deeb)$/pH = 1 TiO_2 (a) and $Ru(en)_2(deeb)$/pH = 12 TiO_2 (b). The solvent was argon-saturated neat acetonitrile for pH = 1 TiO_2 and 0.01 M $LiClO_4$ acetonitrile for pH = 12 TiO_2. The spectra are shown at delay times of 0 ns (■), 200 ns (●), 600 ns (♦) and 2 μs (▲). The absorption difference spectrum from spectroelectrochemistry of $Ru(en)_2(deeb)^{2+}$/pH = 1 TiO_2 (—) normalized to the 200 ns spectrum is overlaid in (a).

Table 5
FT-IR data for compounds in solid-state and anchored to TiO_2.[a].

Compounds	Solid-state (cm^{-1})	TiO_2 (cm^{-1}) pH = 1	pH = 12
$[Ru(NH_3)_5(eina)](PF_6)_2$	1722, 1633, 1603	1722, 1630, 1597	1726, 1593
$[Ru(NH_3)_4(deeb)](PF_6)_2$	1710, 1630, 1603	1722, 1631, 1595	1722, 1593

[a] Frequencies of the COO asymmetric stretch are averages of 64 scans with a resolution of 4 cm^{-1}.

shifted to 1722 cm^{-1} when anchored to TiO_2. The FT-IR spectra of $[Ru(en)_2(deeb)](PF_6)_2$ were qualitatively similar to those of $[Ru(NH_3)_4(deeb)](PF_6)_2$. The FT-IR spectra of the compounds on the acid- and base-pre-treated ZrO_2 thin films were qualitatively the same as those on the respective TiO_2 films. One broad band centered at 1630 cm^{-1} was observed for $[Ru(NH_3)_5(eina)](PF_6)_2$ and $[Ru(NH_3)_4(deeb)](PF_6)_2$ when bound to acid-treated TiO_2, while it was nearly absent on base-treated TiO_2.

There was no evidence for the presence of excited states by nanosecond absorption spectroscopy when the compounds were photo-excited in fluid solution or anchored to metal-oxide supports at room temperature. In fluid acetonitrile solution, steady state illumination resulted in a decrease in the MLCT absorption for all the compounds. No new absorption bands were observed consistent with the loss of the chromophoric deeb or eina ligand and replacement by solvent molecules. The quantum yield for photosolvation of $Ru(NH_3)_5(eina)^{2+}$ in acetonitrile was 0.02 with 489 nm light. Under steady state irradiation at 460 nm, the relative photostability in acetonitrile solution was found to decrease in the order: $Ru(en)_2(deeb)^{2+} > Ru(NH_3)_4(deeb)^{2+} \gg Ru(NH_3)_5(eina)^{2+}$.

Transient absorption difference spectra measured after pulsed-light excitation of $Ru(en)_2(deeb)^{2+}$ anchored to pH = 1 and pH = 12 TiO_2 are shown in Fig. 6a and b. The corresponding spectra of $Ru(NH_3)_4(deeb)/TiO_2$ were very similar to those shown. There was no evidence for the presence of excited states or of ligand-loss photochemistry and the spectra were assigned to an interfacial charge-separated state, $Ru^{III}/TiO_2(e^-)$. The rate of electron injection could not be time-resolved, $k_{inj} > 10^8\ s^{-1}$. Spectroelectrochemistry was employed to generate the absorption spectrum of the oxidized ruthenium compounds that were in turn used to simulate the transient absorption spectra obtained for the acid pre-treated samples. For example, $Ru^{II}(en)_2(deeb)/TiO_2$ was oxidized to $Ru^{III}(en)_2(deeb)/TiO_2$ with an applied potential of +0.95 V vs. Ag/AgCl in 0.1 M $TBAClO_4$ acetonitrile. The absorbance spectrum of

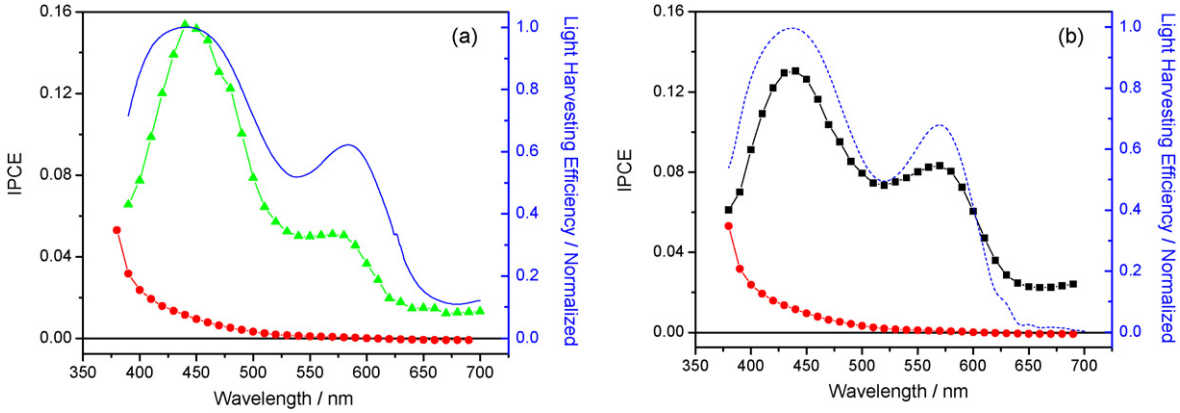

Fig. 7. Photocurrent action spectra of acid pre-treated $Ru(NH_3)_4(deeb)/TiO_2$ (▲) (a) and $Ru(en)_2(deeb)/TiO_2$ (■) (b) in 0.5 M TBAI/0.05 M I_2 acetonitrile solution. The spectra were corrected for the contribution from blank TiO_2 (●). Normalized $1 - T$ spectra for $Ru(NH_3)_4(deeb)/TiO_2$ (▬) (a) and $Ru(en)_2(deeb)/TiO_2$ (▬ ▬ ▬) (b) in 0.5 M $TBAClO_4$ acetonitrile are overlaid on the photocurrent action spectra.

Table 6
Excited-state injection quantum yields, ϕ_{inj}, with 532 and 416 nm light excitation.

Compound	ϕ_{inj} 416 nm	ϕ_{inj} 532 nm
$Ru(NH_3)_5(eina)^{2+}$	0.30 ± 0.05	0.15 ± 0.03
$Ru(NH_3)_4(deeb)^{2+}$	0.38 ± 0.01	0.18 ± 0.04
$Ru(en)_2(deeb)^{2+}$	0.36 ± 0.02	0.22 ± 0.02

the compound in the formal oxidation state of (II) was subtracted from that measured in the (III) state and was scaled and superimposed on the transient data in Fig. 6a as a dashed line. A weak positive absorption was observed at longer observation wavelengths consistent with the presence of $TiO_2(e^-)$, data not shown [2].

Comparative actinometry was utilized to determine the quantum yields (ϕ_{inj}) for excited-state electron injection into TiO_2 [16]. It was assumed that the extinction coefficients of the compounds in fluid solution did not change when anchored to the TiO_2 thin films and that neither the Ru^{III} state nor the injected electron absorbed significantly at the monitoring wavelength, 460 nm. The ϕ_{inj} values were sensitive to the excitation wavelength and the identity of the sensitizer and approximately doubled with 416 nm excitation light relative to 532 nm, Table 6. Surface pre-treatments also had a profound influence on ϕ_{inj}, which was generally several times larger for acid pre-treated films relative to base-treated. The injection yields on base pre-treated TiO_2 could be improved by the addition of $LiClO_4$ to the external acetonitrile.

The recovery of the ground-state absorption quantified at the maximum of the absorption change was well described over the first two microseconds by a second-order, equal-concentration kinetic model, due to $Ru^{III} + TiO_2(e^-)$. The second-order rate constants showed no measurable dependence on the monitoring wavelength, excitation wavelength (416 nm and 532 nm), or irradiance. Typical observed rate constants were on the order of $k_{obs} \sim 5 \times 10^8\ M^{-1}\ s^{-1}$. The $Ru^{III}/TiO_2(e^-)$ charge-separated states returned cleanly to baseline on a millisecond time scale with no evidence for photochemistry after several hundred laser pulses.

Typical photocurrent action spectra of acid pre-treated TiO_2 sensitized with $Ru(NH_3)_4(deeb)^{2+}$ or $Ru(en)_2(deeb)^{2+}$ in 0.5 M TBAI/0.05 M I_2 acetonitrile electrolyte are shown in Fig. 7. The IPCE (incident photon-to-current conversion efficiency) was calculated via Eq. (3):

$$\text{IPCE} = \frac{[1240\ \text{eV nm}][\text{photocurrent density}\ (\text{mA cm}^{-2})]}{[\text{wavelength nm}][\text{irradiance}\ (\text{mW cm}^{-2})]} \quad (3)$$

The maximum IPCE values were ~15%. The photocurrents were lower when dimethylformamide was used in place of CH_3CN. Rapid desorption of sensitizers was observed when LiI was used in place of TBAI. Normalized light harvesting efficiency $(1 - T)$ spectra for $Ru(NH_3)_4(deeb)/TiO_2$ (solid line) and $Ru(en)_2(deeb)/TiO_2$ (dashed line) in 0.5 M $TBAClO_4$ acetonitrile are overlaid on the photocurrent action spectra. No significant photocurrent was observed for $Ru(NH_3)_5(eina)/TiO_2$ under otherwise identical conditions.

4. Discussion

Adsorption isotherm measurements demonstrated that all the ruthenium am(m)ine compounds under study bind strongly to nanocrystalline TiO_2 thin films with adduct formation constants of $1–9 \times 10^5\ M^{-1}$ and surface coverages of $3–10 \times 10^{-8}$ mol/cm^2. The relatively large spread encompasses the fact that TiO_2 films pre-treated with aqueous base solutions gave larger adduct formation constants and surface coverages than those that were untreated or acidic pre-treated [10]. Interestingly, the largest adduct formation constant was measured for $Ru(NH_3)_5(eina)^{2+}$ that contains only a single anchoring ester group. This result appears to be in conflict with a previous report where a significantly lower adduct formation constant was observed for a Ru(II) bipyridyl compound containing a monocarboxy ligand relative to an analogous compound with two [24]. However, the ammine ligands utilized in this study are known to undergo outer-sphere charge transfer interactions and the ester groups were not completely hydrolyzed to their carboxylate forms (see below) [25].

The FT-IR–ATR spectra of the surface-anchored compounds were remarkably similar and insensitive to surface pre-treatments. A single asymmetric COO stretch was observed, 1710–1730 cm^{-1}, and a broad band centered at 1600 cm^{-1}. This similarity indicated a similar binding mode(s) to TiO_2. In previous work with $Ru(deeb)(bpy)_2^{2+}$, FT-IR–ATR data showed quite clearly that the ester groups were hydrolyzed to the carboxylate forms by the TiO_2 surface. This was not the case here and the higher energy band at ~1726 cm^{-1} for the sensitized materials was reasonably assigned to the COO group of the unhydrolyzed, native ester.

Surface attachment was found to induce a 50–300 mV negative shift in the $Ru^{III/II}$ reduction potentials measured relative to the value in fluid electrolyte for both CH_3CN and DMF. The $Ru^{III/II}$ reduction potentials were solvent dependent and were more negative in DMF electrolytes than in acetonitrile [4]. For heteroleptic ruthenium polypyridyl compounds, comparative studies have shown that the $Ru^{III/II}$ reduction potentials were the same, to within 50 mV, in solution and when the compounds were bound to TiO_2. However, metal ammine and cyano compounds are well known to be much more sensitive to the local environment than are tris-chelated compounds. Outer-sphere interactions with ammine and cyano ligands have a significant influence on $M^{III/II}$ potentials and this underlies the significant solvatochromism observed with this class of compounds. A related study with the highly solvatochromic compound $Ru(dcb)(CN)_4^{2-}$, also revealed a more negative $Ru^{III/II}$ reduction potential relative to that in fluid solution [26]. For the am(m)ine compounds under study, the surface-induced cathodic shift is most likely due to hydrogen bond formation between ammine protons and surface oxygen atoms of the polar TiO_2 interface [27]. An infrared study on similar anatase TiO_2 thin films provided spectroscopic evidence for the presence of surface bound-OH_2^+ species at acidic surfaces [28].

The $Ru^{III/II}$ reduction potentials showed a 70–90 mV anodic shift on pH = 12 TiO_2 relative to those on pH = 1 TiO_2. Zaban and coworkers reported that $Ru^{III/II}$ reduction potential shifts induced by semiconductor surface acidity varied from 21 mV to 53 mV per pH unit depending on whether the physical location of the sensitizer was inside or outside the double layer [29]. The small shift observed here is in agreement with a previous report using the same sample pre-treatment procedures [13].

In fluid solution the ligand reduction potentials were observed to be less solvent dependent, shifting ~100 mV cathodically. If this behavior was translated to the semiconductor surface, the surface-induced $Ru^{III/II}$ reduction potential shift would increase the spectral response of the materials at long wavelengths and alter the driving force for iodide oxidation. Indeed, solvatochromic dye-sensitized nanocrystalline solar cells have recently been reported [25]. Compared to the $Ru^{III/II}$ reduction potential of $Ru(NH_3)_5(eina)^{2+}$, those of $Ru(NH_3)_4(deeb)^{2+}$ and $Ru(en)_2(deeb)^{2+}$ are considerably more positive and are closer to the widely used sensitizer *cis*-$Ru(dcb)_2(NCS)_2$, 0.85 V vs. SCE in fluid acetonitrile [30].

The photophysical and photochemical properties of ruthenium ammine compounds have been extensively investigated [4,5]. The visible spectra are characterized by MLCT absorptions that are solvent dependent. The properties of the excited state are dominated by the presence of a low-lying LF state. Therefore, ruthenium ammine excited states typically have picoseconds lifetimes and are photolabile in fluid solution. Recently, a systematic study of the 77 K emission of a series of $[Ru(Am)_{6-2n}(bpy)_n]^{2+}$ compounds (n = 1–3),

where Am is an am(m)ine, has been reported [15,17]. The emission energies were observed to decrease as n increased in good correlation with electrochemical oxidation and reduction potentials in ambient solutions. In preliminary studies, the energy of the 77 K MLCT emission of $Ru(en)_2(deeb)^{2+}$ in butyronitrile glass was found to be ~11,400 cm^{-1}, consistent with the variations in the differences in metal and ligand reduction potentials. The very small amplitude envelope of medium frequency vibronic components, *i.e.* ~1300 cm^{-1}, is most likely an attenuation effect that arises from configurational mixing with the ground state. Most of this probably comes from the shift of the ground state potential energy minimum.

Previous studies have indicated that the σ-donating and π-back-bonding properties of the ligand influence the MLCT excited-state energies in ruthenium polypyridyl compounds [31]. The electron-withdrawing diethyl ester groups on deeb ligands stabilize the π^* levels of bipyridine, resulting in a red-shifted MLCT emission for $Ru(deeb)_3^{2+}$, relative to the $Ru(bpy)_3^{2+}$. If this behavior translates to ruthenium ammine compounds in the frozen butyronitrile glass at 77 K, a red-shifted MLCT emission for $Ru(NH_3)_4(deeb)^{2+}$, relative to $Ru(NH_3)_4(bpy)^{2+}$ is expected. Not surprising, the emission energies at 77 K for $Ru(en)_2(deeb)^{2+}$ red-shifted ~1650 cm^{-1} relative to those reported for $Ru(NH_3)_4(bpy)^{2+}$ [17].

Gerischer theory predicts that the excited-state injection rate constant, k_{inj}, is related to the product of the transfer frequency and overlap of the excited-state donor levels and TiO_2 acceptor states integrated over all energies, Eq. (4),

$$k_{inj} \sim \int \kappa(E) D_a(E) W_d(E)\, dE \quad (4)$$

where $\kappa(E)$ is the transfer frequency, $D_a(E)$ is the density of unoccupied acceptor states in TiO_2, and $W_d(E)$ is the sensitizer excited-state donor distribution function [32]. A number a studies have indicated that $D_a(E)$ increases exponentially toward the vacuum level in these nanocrystalline thin films [33]. Therefore, the injection rate constant is expected to be sensitive to the excited-state reduction potential, $E^0(Ru^{III/II*})$, and is optimized for sensitizers that are stronger photoreductants, *i.e.* possess more negative excited-state potentials. The injection quantum yields for the three compounds were at most 0.38, although electrochemical and photoluminescence studies of $Ru(en)_2(deeb)^{2+}$ indicated that the photoluminescent excited state was a potent photoreductant that possessed strong overlap with the TiO_2 acceptor states. Injection occurring from vibrationally hot excited states or singlet excited states is necessarily more energetically favorable [34]. In the limit of excited-state injection from the initially formed Franck–Condon excited state, the energy of the absorbed photon directly determines the excited-state reducing power, Eq. (2) with $\Delta G_{es} = h\nu$. The higher injection yields measured for blue light excitation relative to green light clearly indicates that some injection is occurring from upper excited states. The poor overall injection quantum yields were attributed to competitive rapid internal conversion and non-radiative decay processes that are absent in the Ru(II) sensitizers commonly utilized for solar energy conversion applications.

The photocurrent data provide further evidence that electron injection occurs in part from non-thermally-equilibrated excited states [3]. The incident photon-to-current efficiency, IPCE, is proportional to three terms: the absorptance or light harvesting efficiency (LHE), the injection quantum yield (ϕ_{inj}) and the efficiency with which injected electrons are collected in the external circuit (η_{coll}), Eq. (5),

$$IPCE = LHE\, \phi_{inj}\, \eta_{coll} \quad (5)$$

The wavelength dependence of the IPCE is normally attributed to the LHE of the sensitizer, which is equivalent to the absorptance, and, in the absence of light scattering, one minus the transmittance ($1 - T$). However, comparisons of the photocurrent action spectra of $Ru(NH_3)_4(deeb)^{2+}$ and $Ru(en)_2(deeb)^{2+}$ with their $1 - T$ spectra reveal that the decreased photocurrent observed at longer wavelengths cannot be solely explained by decreased light absorption or by direct excitation of the TiO_2. Instead, this must reflect a wavelength dependence of either ϕ_{inj}, η_{coll}, or both. The collection efficiency could be wavelength dependent if electrons injected further away from the conductive glass FTO substrate have a higher probability of undergoing recombination. Since control experiments with other ruthenium polypyridyl sensitizers, such as $Ru(bpy)_2(deeb)^{2+}$, exhibited coincident photocurrent action and absorptance spectra at these photon energies, the dissimilarity between the photocurrent and absorptance spectra observed here most likely reflect a wavelength-dependent injection yield. This conclusion is also consistent with the comparative actinometry measurements made at open circuit in the absence of the redox mediator. To our knowledge, there are only four previous reports of photocurrent action spectra that did not correspond to the sensitizer absorptance spectrum and these authors also concluded that this behavior resulted from wavelength-dependent excited-state injection [2b,3a,d,35].

In previous work, a ruthenium penta-ammine compound with a single chromophoric pyridine ligand, $[Ru(NH_3)_5(eina)](PF_6)_2$, was successfully utilized to sensitize nanocrystalline TiO_2 thin films [6c]. Comparative actinometry measurements indicated that the interfacial electron-injection quantum yield, ϕ_{inj}, was excitation-wavelength dependent and sensitive to deuteration of the ammines. The quantum yields were optimized with blue light excitation (416 nm) and complete deuterium substitution [6d]. These results also indicated that electron injection occurs in competition with excited-state vibrational relaxation and/or intersystem crossing. In regenerative solar cells employing $Ru(NH_3)_5(eina)^{2+}$, negligibly small photocurrents were measured while the sensitizers reported here gave incident photon-to-current efficiencies as high as 15%. This undoubtedly reflects the more positive $Ru^{III/II}$ reduction potentials. After excited state injection, the sensitizer is present in the Ru(III) formal oxidation state and must oxidize iodide before recombination with the injected electron. If iodide oxidation is slow, the injected electron will recombine with the oxidized sensitizer and no measureable steady state photocurrent results. Sensitizers with more positive $Ru^{III/II}$ reduction are expected to oxidize iodide more efficiently and hence give larger photocurrents as was observed here. However, the potentials still remain to be optimized for iodide oxidation such that recombination with the oxidized sensitizer is negligible [36]. The $Ru^{III/II}$ reduction potentials of the new sensitizers reported here are ~200 mV negative of that measured for optimized sensitized materials such as Z907/TiO_2 [37]. Thus some losses are expected in η_{coll} due to rapid $TiO_2(e^-)$ + Ru(III) recombination. Indeed the fact that the IPCE values are a factor of two lower than the measured injection yields probably reflects this.

5. Conclusions

Two new ruthenium am(m)ine bipyridyl compounds were prepared, characterized, and found to sensitize nanocrystalline TiO_2 thin films to visible light. The excited states injected electrons into TiO_2 rapidly, $k_{inj} > 10^8\ s^{-1}$, but the yield was found to be excitation wavelength dependent. In regenerative solar cells, light absorption by the higher energy MLCT absorption band resulted in a larger photocurrent than did light absorption by the lower energy MLCT band. The results suggest that the presence of low-lying ligand field states results in an excited state deactivation pathway that competes kinetically with electron injection.

Acknowledgements

The National Science Foundation is gratefully acknowledged for support of this work. We would also like to thank Dr. O.S. Odongo and Prof. John F. Endicott for the emission spectra and for many thoughtful discussions.

References

[1] (a) Y. Tachibana, J.E. Moser, M. Grätzel, D.R. Klug, J.R. Durrant, J. Phys. Chem. 100 (1996) 20056;
(b) T. Hannappel, B. Burfeindt, W. Storck, F. Willig, J. Phys. Chem. B 101 (1997) 6799;
(c) J.B. Asbury, R.J. Ellingson, H.N. Ghosh, S. Ferrere, A.J. Nozik, T. Lian, J. Phys. Chem. B 103 (1999) 3110;
(d) G. Benko, J. Kallioinen, J.E.I. Korppi-Tommola, A.P. Yartsev, V. Sundström, J. Am. Chem. Soc. 124 (2002) 489;
(e) D. Kuciauskas, J.E. Monat, R. Villahermosa, H.B. Gray, N.S. Lewis, J.K. McCusker, J. Phys. Chem. B 106 (2002) 9347;
(f) M.I. Ranasinghe, Y. Wang, T. Goodson III, J. Am. Chem. Soc. 125 (2003) 5258;
(g) N.A. Anderson, T. Lian, Coord. Chem. Rev. 248 (2004) 1231;
(h) S.A. Haque, E. Palomares, B.M. Cho, A.N.M. Green, N. Hirata, D.R. Klug, J.R. Durrant, J. Am. Chem. Soc. 127 (2005) 3456;
(i) D.F. Watson, G.J. Meyer, Annu. Rev. Phys. Chem. 56 (2005) 119;
(j) A. Furube, R. Katoh, K. Hara, T. Sato, S. Murata, H. Arakawa, M. Tachiya, J. Phys. Chem. B 109 (2005) 16406;
(k) J. Huang, D. Stockwell, A. Boulesbaa, J. Guo, T. Lian, J. Phys. Chem. C 112 (2008) 5203;
(l) P. Myllyperkiö, G. Benkő, J. Korppi-Tommola, A.P. Yartsev, V. Sundström, Phys. Chem. Chem. Phys. 10 (2008) 996;
(m) S.E. Koops, B.C. O'Regan, P.R.F. Barnes, J.R. Durrant, J. Am. Chem. Soc. 131 (2009) 4808;
(n) A. Furube, Z.-S. Wang, K. Sunahara, K. Hara, R. Katoh, M. Tachiya, J. Am. Chem. Soc. 132 (2010) 6614.
[2] (a) J.-E. Moser, M. Grätzel, Chimia 52 (1998) 160;
(b) A. Islam, K. Hara, L.P. Singh, R. Katoh, M. Yanagida, S. Murata, Y. Takahashi, H. Sugihara, H. Arakawa, Chem. Lett 29 (2000) 490;
(c) F. Lenzmann, J. Krueger, S. Burnside, K. Brooks, M. Grätzel, D. Gal, S. Rühle, D. Cahen, J. Phys. Chem. B 105 (2001) 6347;
(d) J.K. McCusker, Acc. Chem. Res. 36 (2003) 876;
(e) G.J. Meyer, Inorg. Chem. 44 (2005) 6852;
(f) S. Ardo, G.J. Meyer, Chem. Soc. Rev. 38 (2009) 115.
[3] (a) S. Ferrere, B.A. Gregg, J. Am. Chem. Soc. 120 (1998) 843;
(b) S. Ferrere, Chem. Mater. 12 (2000) 1083;
(c) J.E. Monat, J.K. McCusker, J. Am. Chem. Soc. 122 (2000) 4092;
(d) M. Yang, D.W. Thompson, G.J. Meyer, Inorg. Chem. 41 (2002) 1254;
(e) H.-L. Xai, S. Ardo, A.A. Narducci Sarjeant, S. Huang, G.J. Meyer, Langmuir 25 (2009) 13641.
[4] (a) G. Malouf, P.C. Ford, J. Am. Chem. Soc. 96 (1974) 601;
(b) G. Malouf, P.C. Ford, J. Am. Chem. Soc. 99 (1977) 7213;
(c) V.A. Durante, P.C. Ford, Inorg. Chem. 18 (1979) 588;
(d) R.-g.M. Carlos, M.G. Neumann, E. Tfouni, Inorg. Chem. 35 (1996) 2229;
(e) Y.K. Shin, B.S. Brunschwig, C. Creutz, M.D. Newton, N. Sutin, J. Phys. Chem. 100 (1996) 1104;
(f) N.V. Ivanova, V.V. Sizov, A.B. Nikolskii, A.I. Panin, J. Struct. Chem. 40 (1999) 620.
[5] (a) Y.C. Chung, N. Leventis, P.J. Wagner, G.E. Leroi, J. Am. Chem. Soc. 107 (1985) 1414;
(b) J.R. Winkler, T.L. Netzel, C. Creutz, N. Sutin, J. Am. Chem. Soc. 109 (1987) 2381.
[6] (a) P. Qu, D.W. Thompson, G.J. Meyer, Langmuir 16 (2000) 4662;
(b) C.A. Kelly, G.J. Meyer, Coord. Chem. Rev. 211 (2001) 295;
(c) F. Liu, G.J. Meyer, Inorg. Chem. 42 (2003) 7351;
(d) F. Liu, G.J. Meyer, J. Am. Chem. Soc. 127 (2005) 824;
(e) F. Liu, G.J. Meyer, Inorg. Chem. 44 (2005) 9305.
[7] A.R. Oki, R.J. Morgan, Synth. Commun. 25 (1995) 4093.
[8] L.H. Vogt Jr., J.L. Katz, S.E. Wiberley, Inorg. Chem. 4 (1965) 1157.
[9] F. Liu, M. Yang, G.J. Meyer, in: S. Sakka (Ed.), In Handbook of Sol–Gel Science and Technology, vol. 2, Kluwer Academic Publishers, Netherlands, 2005, p. 399.
[10] P. Qu, G.J. Meyer, Langmuir 17 (2001) 6720.
[11] P.C. Ford, F.P. De, R. Rudd, H. Gaunder, Taube, J. Am. Chem. Soc. 90 (1968) 1187.
[12] S.K. Doorn, J.T. Hupp, J. Am. Chem. Soc. 111 (1989) 4704.
[13] (a) J.A. Broomhead, L.A.P. Kane-Maguire, J. Chem. Soc. (1967) 546;
(b) J.K. Witschy, J.K. Beattie, Inorg. Nucl. Chem. Lett. 5 (1969) 969;
(c) D.F. Mahoney, J.K. Beattie, Inorg. Chem. 12 (1973) 2561.
[14] (a) J.R. Schoonover, J. Ni, L. Roecker, P.S. White, T.J. Meyer, Inorg. Chem. 35 (1996) 5885;
(b) V.J. Catalano, R.A. Heck, C.E. Immoos, A. Ohman, M.G. Hill, Inorg. Chem. 37 (1998) 2150.
[15] P. Xie, Y.-J. Chen, Md.J. Uddin, J.F. Endicott, J. Phys. Chem. A 109 (2005) 4671.
[16] B.V. Bergeron, C.A. Kelly, G.J. Meyer, Langmuir 19 (2003) 8389.
[17] (a) P. Xie, Y.-J. Chen, J.F. Endicott, Md.J. Uddin, D. Seneviratne, P.G. McNamara, Inorg. Chem. 42 (2003) 5040;
(b) Y.J. Chen, P. Xie, M.J. Heeg, J.F. Endicott, Inorg. Chem. 45 (2006) 6282.
[18] (a) S.J. Hug, S.G. Boxer, Inorg. Chim. Acta 242 (1996) 323;
(b) J.H. Streiff, W.D. Edwards, J.L. McHale, Chem. Phys. Lett. 312 (1999) 369;
(c) D.S. Seneviratne, Md.J. Uddin, V. Swayambunathan, H.B. Schlegel, J.F. Endicott, Inorg. Chem. 41 (2002) 1502.
[19] G.M. Pearl, M.C. Zerner, J. Am. Chem. Soc 121 (1999) 399.
[20] (a) Y.-J. Chen, P.G. McNamara, J.F. Endicott, J. Phys. Chem. B 111 (2007) 6748;
(b) Y.-J. Chen, P. Xie, J.F. Endicott, J. Phys. Chem. A 108 (2004) 5041;
(c) J.F. Endicott, Y.-J. Chen, P. Xie, Coord. Chem. Rev. 249 (2005) 343;
(d) J.F. Endicott, P.G. McNamara, T. Buranda, A.V. Macatangay, Coord. Chem. Rev. 208 (2000) 61;
(e) Y.-J. Chen, O.S. Odongo, P.G. McNamara, K.T. Szacilowski, J.F. Endicott, Inorg. Chem. 47 (2008) 10921.
[21] H. Kobayashi, Y. Kaizu, Coord. Chem. Rev. 64 (1985) 53.
[22] A.J. Bard, L.R. Faulkner, Electrochemical Methods: Fundamentals and Applications, 2nd ed., John Wiley & Sons, New York, 2001.
[23] (a) D. Rehm, A. Weller, Ber. Bunsen. Phys. Chem. 73 (1969) 834;
(b) D. Rehm, A. Weller, Israel J. Chem. 8 (1970) 259;
(c) C.R. Bock, J.A. Connor, A.R. Gutierrez, T.J. Meyer, D.G. Whitten, B.P. Sullivan, J.K. Nagle, J. Am. Chem. Soc. 101 (1979) 4815;
(d) C.R. Bock, T.J. Meyer, D.G. Whitten, J. Am. Chem. Soc. 97 (1975) 2909.
[24] K. Kilså, E.I. Mayo, B.S. Brunschwig, H.B. Gray, N.S. Lewis, J.R. Winkler, J. Phys. Chem. B 108 (2004) 15640.
[25] P. Chen, T.J. Meyer, Chem. Rev. 98 (1998) 1439.
[26] R. Argazzi, C.A. Bignozzi, M. Yang, G.M. Hasselmann, G.J. Meyer, Nano. Lett. 2 (2002) 625.
[27] (a) E.M. Kober, B.P. Sullivan, T.J. Meyer, Inorg. Chem. 23 (1984) 2098;
(b) J. Streiff, J.L. McHale, J. Chem. Phys. 112 (2000) 841.
[28] P.A. Connor, K.D. Dobson, A.J. McQuillan, Langmuir 15 (1999) 2402.
[29] (a) A. Zaban, S. Ferrere, J. Sprague, B.A. Gregg, J. Phys. Chem. B 101 (1997) 55;
(b) A. Zaban, S. Ferrere, B.A. Gregg, J. Phys. Chem. B 102 (1998) 452.
[30] M.K. Nazeeruddin, A. Kay, I. Rodicio, R. Humphry-Baker, E. Muller, P. Liska, N. Vlachopoulos, M. Grätzel, J. Am. Chem. Soc. 115 (1993) 6382.
[31] A. Juris, V. Balzani, F. Barigelletti, S. Campagna, P. Belser, A. von Zelewsky, Coord. Chem. Rev. 84 (1988) 85.
[32] (a) H. Gerischer, Surf. Sci. 18 (1969) 97;
(b) H. Gerischer, Pure Appl. Chem. 52 (1980) 2649.
[33] (a) F. Fabregat-Santiago, I. Mora-Seró, G. Garcia-Belmonte, J. Bisquert, J. Phys. Chem. B 107 (2003) 758;
(b) M. Bailes, P.J. Cameron, K. Lobato, L.M. Peter, J. Phys. Chem. B 109 (2005) 15429;
(c) I. Abayev, A. Zaban, V.G. Kytin, A.A. Danilin, G. Garcia-Belmonte, J. Bisquert, J. Solid State Electrochem. 11 (2007) 647;
(d) A.J. Morris, G.J. Meyer, J. Phys. Chem. C 112 (2008) 18224.
[34] (a) P.G. Hoertz, D.W. Thompson, L.A. Friedman, G.J. Meyer, J. Am. Chem. Soc. 124 (2002) 9690;
(b) P.G. Hoertz, A. Staniszewski, A. Marton, G.T. Higgins, C.D. Incarvito, A.L. Rheingold, G.J. Meyer, J. Am. Chem. Soc. 128 (2006) 8234.
[35] T.A. Heimer, E.J. Heilweil, C.A. Bignozzi, G.J. Meyer, J. Phys. Chem. A 104 (2000) 4256.
[36] (a) J.M. Gardner, J.M. Giaimuccio, G.J. Meyer, J. Am. Chem. Soc. 130 (2008) 17252;
(b) J.M. Gardner, M. Abrahamsson, B. Farnum, G.J. Meyer, J. Am. Chem. Soc. 131 (2009) 16206;
(c) X. Wang, D.M. Stanbury, Inorg. Chem. 45 (2006) 3415;
(d) G. Boschloo, A. Hagfeldt, Acc. Chem. Res. 42 (2009) 1819.
[37] Md.K. Nazeeruddin, S.M. Zakeeruddin, J.-J. Lagref, P. Liska, P. Comte, C. Barolo, G. Viscardi, K. Schenk, M. Grätzel, Coord. Chem. Rev. 248 (2004) 1317.